



**LIGATIONAL AND SPECTROSCOPIC ON SOME SULFAMETHOXAZOLE
METAL COMPLEXES AS ANTIMICROBIAL AGENTS**

Yasmin M.S. Jamil, Maher Ali Al-Maqtari* and Mohammed K. Al-Qadasi

Department of Chemistry, Faculty of Science, Sana'a University.

*Corresponding Author: Dr. Maher Ali Al-Maqtari

Department of Chemistry, Faculty of Science, Sana'a University.

Article Received on 03/05/2017

Article Revised on 23/05/2017

Article Accepted on 12/06/2017

ABSTRACT

Metal complexes have been applied as medicinal agents in the treatment of different human infections and diseases. So, the aim of this study is focused on studying the ligational, spectroscopic and evaluating antimicrobial investigations of sulfamethoxazole (SMX) drug complexes formulas with Mn (II), Cu (II), Ni (II), Zn (II), Y(III), La(III), Nd(III) and Gd(III) metal ions. These complexes with sulfamethoxazole ligand as to evaluate the biological activity were synthesized and characterized by elemental analysis, molar conductance, magnetic susceptibility, UV-vis, IR and ¹H-NMR spectroscopy. The IR spectral data suggested that the coordination sites of SMX are the sulfonyloxygen and SO₂-NH sulfonamide nitrogen as a bidentate ligand, from the microanalytical data, the stoichiometry of the complexes 1:2 (metal: ligand) was found, and the morphological nano structures of SMX complexes were checked using X-ray powder diffraction (XRD) and scanning electron microscope (SEM). The metal complexes were screened for antibacterial activity against Gram-ve (*Escherichia coli*) (ATCC 8739) and Gram+ve (*Staphylococcus aureus*) (ATCC 8739) and antifungal (*Aspergillus flavus*) (ATCC 9643) and *Aspergillus fumigatus* (ATCC 1022). These complexes considered in this research showed as a satisfactory antimicrobial activity.

KEYWORDS: Sulfamethoxazole, lanthanides, nano size, antimicrobial activity.

1. INTRODUCTION

Sulfamethoxazole (4-amino-N-(5-methyl-3-isoxazolyl)-benzenesulfonamide; (SMX) (Figure 1) is the most predominant sulfonamide in human medicine. It is a bacteriostatic antibiotic.^[1] It is most often used as part of a synergistic combination. Sulfonamides are synthetic antimicrobial agents derived from sulfanilamide, whose antibacterial activity was discovered in the early 1930's by Domagk and Tréfouel.^[2-4] Especially in the case of penicillin's hypersensitivity, sulfonamides were prescribed against a wide variety of bacterial infections. This is due to the fact that they interfere with p-aminobenzoic acid (PABA) in the biosynthesis of tetrahydrofolic acid, which is essential for the metabolic process of bacteria.^[5] Also, some sulfa drugs were used in the treatment of cancer, malaria, leprosy and tuberculosis.^[6] However, the widespread bacterial resistance to these compounds limits their application spectrum today. The realization of the interaction between biologically active molecules and metals is extremely important. Such interactions occupy prominence in the field of medicinal inorganic chemistry where it is offer great possibilities in biomaterials

preparation process, considering certain aspects of biocompatibility or even in design of therapeutic agents which are not readily available to organic compounds.^[1,7,8] Actually, therapeutic value of the metal drug complexes has encouraged the researcher to improve on new alternative drugs.^[9,10] In our case, the presence of donor atoms (N, S, O) at various positions in SMX molecule enable it to behave as multidentate ligand and thus form chelates of diverse structural types with a wide range of metal ions.^[11] In addition to sulfa drugs, other drugs show the same behavior when it chelate with metal ions studied in present work.^[12-19] In literature survey, many authors have been reported the antimicrobial activity of sulfa drugs and their metal complexes.^[20-24] The metal sulfa-drugs chelates have a great pharmacological, physiological and more bacteriostatic rather than their free drugs itself.^[23-26] In this article, the coordination mode of sulfamethoxazole chelating via Mn (II), Cu (II), Ni (II), Zn (II), Y(III), La(III), Nd(III) and Gd(III) metal ions have been investigated. The antimicrobial activities of these complexes were also evaluated upon their nanometric behavior.

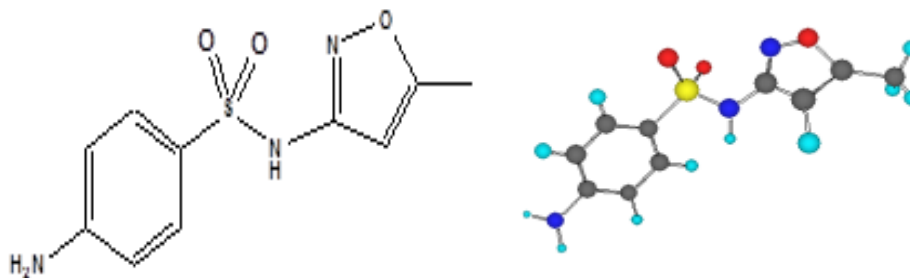


Figure: 1 Sulfamethoxazole (SMX) drug

2. Experimental

2.1. Materials

All chemicals, solvents, indicators, metal(II) chlorides (i.e. manganese, copper, nickel and zinc) hydrate and metal(III) chlorides (i.e. yttrium, lanthanum, neodymium and gadolinium) hydrate were commercially available from BDH and were used without further purification. The standard pure drug (Sulfamethoxazole) was presented from MODERN PHARMA Company at Yemen. The Sulfamethoxazole used is a white or almost white crystalline powder with melting point of 169–172°C. This powder is practically insoluble in water, freely soluble in methanol and acetone, slightly soluble in ether. It dissolves in dilute solutions of sodium hydroxide.^[27]

2.2. Preparation of the drug metal complexes

All the interested complexes under investigation were prepared similarly according to the following procedure: In general, 4 mmol of sulfamethoxazole ligand was dissolved in 25 mL methanol then mixed with 25 mL of methanolic solution of 2 mmol metal chloride of Mn (II), Cu (II), Ni (II), Zn (II), Y(III), La(III), Nd(III) or Gd(III). Mixtures with molar ratio of 1:2 ($MCl_{2 \text{ or } 3} \cdot xH_2O$: ligand), were refluxed with continuous stirring at 60–70°C for about 3 h. The mixtures were left overnight until precipitated. The precipitates obtained were filtered off and washed several times using methanol then left over anhydrous calcium chloride. The yield percent of each product collected were about 55–70%.

2.3. Spectral measurements

IR spectra of the metal complexes were recorded on TASCOCO-FT/IR-410 spectrophotometer using the KBr technique, in the region 4000–400 cm^{-1} , at Sana'a University. The electronic spectra of the complexes were measured in DMSO solvent with concentration of 1×10^{-3} M, in range 200–1100 nm by using SPECORD 200/analytic Jenaspectrometer, at Sana'a University. The proton NMR spectra were recorded on a Varian FT-300 MHz spectrometer in d_6 -DMSO solvent, using TMS as internal standard (at Cairo University, Giza, Egypt). SEM images were obtained using a Jeol Jem-1200 EX II Electron Microscope at an acceleration voltage of 25 kV. The samples were coated with a gold plate, at Ain Shams University. X-ray diffraction (XRD) patterns of the samples were recorded on a X Pert Philips X-ray diffractometer. All the diffraction patterns were obtained

by using $Cu K_{\alpha 1}$ radiation, with a graphite monochromator at 0.02°/min scanning rate. The metal complexes were made in the form of tablets, which have ~ 0.1 cm thickness, under a pressure of approximately 5×10^7 Pa, at Ain Shams University.

2.4. Microanalytical analysis

Carbon, hydrogen, nitrogen and sulfur of the complexes have been carried out in Vario EL Fab. CHNS Nr.11042023, at Central Laboratory, Faculty of Science, Ain Shams University, Egypt. The metal and chloride content percentage were determined by titration methods, and water percentage was determined by gravimetric method.^[28]

2.5. Molar conductance

The molar conductance of 10^{-3} M solutions of the SMX ligand and their metal complexes in DMF solvent were measured on a HACH conductivity meter model. All the measurements were taken at room temperature for freshly prepared solutions.

2.6. Melting point measurements

Stuart Scientific electro thermal melting point apparatus was used to measure the melting points of the ligands and their metal complexes in glass capillary tubes in degrees Celsius.

2.7. Magnetic measurements

The mass susceptibility (X_g) of the solid complexes was measured at room temperature using Gouy's method by a magnetic susceptibility balance from Johnson Matthey and Sherwood model, at Cairo University Central Lab. The effective magnetic moment (μ_{eff}) values were obtained using the following Eqs. (1-3).^[29]

$$X_g = \frac{C_{\text{Bal}} L (R - R_0)}{10^9 M} \quad (1)$$

Where:

R_0 is the reading of empty tube, L is the sample length (cm), M is the sample mass (g), R is the reading for tube with sample, C_{Bal} is the balance calibration constant = 2.086.

$$X_M = X_g \times M \cdot Wt. \quad (2)$$

The values of X_M as calculated from equation (2) are corrected for the diamagnetism of the ligand using Pascal's constants, and then applied in Curie's equation (3).

$$\mu_{eff} = 2.84 \sqrt{X_M \times T} \quad (3)$$

Where $T = t (^{\circ}\text{C}) + 273$

2.8. Biological screening

The sulfamethoxazole ligand and their metal complexes were tested for their antimicrobial activity against two species of bacteria (*S. aureus*, and *E. coli*) and two fungal species (*A. flavus* and *A. fumigatus*) using filter disc diffusion method [30]. The screened compounds were dissolved individually in DMSO (dimethylsulfoxide) in order to make up a solution of 50 mg/mL concentration for each of these compounds. The paper discs impregnated with 10 μl of the test samples were placed on the solidified medium as Muller Hilton Agar (MHA) and Sabouraud Dextrose Agar (SDA) for bacterial and fungal, respectively. The plates were pre-incubated for 1 h at room temperature and incubated at 37 $^{\circ}\text{C}$ for 24 h. and at 28 $^{\circ}\text{C}$ for 7 days for antibacterial and antifungal activity test respectively. The diameters of inhibition zones (mm) were measured at the end of an incubation period. Discs saturated with DMSO are used as solvent control.

3. RESULTS AND DISCUSSION

The metal complexes of sulfamethoxazole with Mn (II), Cu (II), Ni (II), Zn (II), Y(III), La(III), Nd(III) and Gd(III) were synthesized. Some physical properties and analytical data of these eight complexes were summarized in (Table 1). The complexes are colored, microcrystalline, quite stable in air and possess slightly high melting points. The analytical data given in Table 1 are in good agreement with the formulas proposed of 1:2 (metal:SMX) molar ratio. These complexes were partially soluble in hot methanol, dimethylsulfoxide and dimethylformamide, but insoluble in water and some other organic solvents. A close examination of molar conductance values of these complexes reveals that the chelates have low conductivity, which indicates nonelectrolytic nature of the complexes. The suggested formula structures of the complexes were based on the results of the elemental analyses, molar conductivity, (infrared and UV-visible) spectra, ^1H NMR, effective magnetic moment in Bohr magnetons, and characterized by X-ray powder diffraction (XRD) and scanning electron microscopy (SEM).

Table 1: Elemental analyses and physical data of the SMX complexes

Complex	color	m.p. $^{\circ}\text{C}$	Elemental analysis (found/calcd), %						Λ_M , mhos cm^2/mol
			C	H	N	S	Cl	M	
[MnL ₂ Cl ₂].2H ₂ O	Paige	185	35.94/ (1)	3.92/ 4.01	12.57/ 12.33	9.59/ 9.62	10.61/ 10.82	8.22/ 8.50	16.68
[NiL ₂ Cl ₂].3H ₂ O	green	218	34.80/ (2)	4.09/ 3.92	12.18/ 12.22	9.29/ 9.25	10.27/ 10.32	8.50/ 8.61	17.11
[CuL ₂ Cl ₂].3H ₂ O	brown	237	34.56/ (3)	4.06/ 4.00	12.09/ 12.02	9.23/ 9.46	10.20/ 10.25	9.14/ 9.30	11.15
[ZnL ₂ Cl ₂].2H ₂ O	white	198	35.38/ (4)	3.86/ 3.91	12.38/ 12.31	9.45/ 9.21	10.44/ 10.50	9.63/ 9.80	13.24
[LaL ₂ Cl ₃].3H ₂ O	white	>300	29.81/ (5)	3.50/ 3.34	10.43/ 10.32	7.96/ 8.12	13.20/ 13.32	17.24/ 17.02	12.45
[NdL ₂ Cl ₃].2H ₂ O	pink	280	30.29/ (6)	3.30/ 3.45	10.60/ 10.61	8.09/ 8.11	13.41/ 13.56	18.18/ 17.96	7.11
[GdL ₂ Cl ₃].H ₂ O	white	253	29.48 (7)	3.07/ 3.11	10.66/ 10.54	8.14/ 8.12	13.49/ 13.43	19.95/ 19.95	8.85
[YL ₂ Cl ₃].3H ₂ O	white	>300	31.78 (8)	3.73/ 3.64	11.12/ 11.14	8.48/ 8.49	14.07/ 14.15	11.76/ 11.80	13.41

3.1 Infrared spectra

The tentative assignments of the peaks for SMX together with metals as a metal complexes are listed in (Table 2). SMX is a positional ligand which may act as a bidentate or tridentate as illustrate by its structure so it expected that IR measurements are highly indicating with respect to the complexation behavior with various metal ions. Infrared spectrum of the free ligand (Figure 2) shows two strong bands at 3468 and 3375 cm^{-1} corresponding to the asymmetric and symmetric stretching vibrations, respectively of the aromatic amino group.^[31] The medium and strong band which appeared at 3298 cm^{-1} is due to the presence of asymmetric sulfonamide $-\text{NH}$ and a weak band at 3242 cm^{-1} as symmetric frequency. Another band observed at 1645 cm^{-1} is related to methoxazole ring stretching vibration.

Others two bands appeared at 1365 and 1188 cm^{-1} are due to asymmetric and symmetric stretching frequencies of sulfonyl group.^[31] The stretching frequencies of the C–N band of sulfonamide is exhibited in the 1311 cm^{-1} region. The spectrum also shows another medium band at (1597 cm^{-1}) which assigned to the stretching frequency of (C=C) band, while the bands appeared at (829, and 686 cm^{-1}) may be assigned to the bending of (S-O) group.^[32] The multiband and shifting of sulfonamide $-\text{NH}$ in the spectra of the prepared complexes (Fig 3a and b), indicating the involvement of this group in chelation with central metal ion by nitrogen of this group according to the data reported in literature.^[32] The band related to methoxazole ring stretching vibrations suffered a very slight shift in range of $\pm 5\text{cm}^{-1}$ in the spectra of the metal complexes indicating that the methoxazole moiety

is not participation in coordination with metal ions.^[33] The bands corresponding to asymmetric of sulfonyl group undergoes a shift toward higher frequencies which observed at (1373-1385) cm^{-1} , while a small bands of the symmetric stretching suffered of a shift toward lower frequencies about (27- 41) cm^{-1} in all complexes. According to these results, the coordination mode of this ligand with metal ions is clearly predicted as a bidentate through the O,N atoms of sulfonamid group for all

complexes, more evidence new bands which appeared in the range (474-521) cm^{-1} ,(411-443) and (260-275) cm^{-1} due to the stretching frequencies of (M-O), (M-N) and (M-Cl) bonds, respectively [34].The presence of water molecules outside the coordination sphere is indicated by a broad band in the region of 3500–3550 cm^{-1} . This is further confirmed by the appearance of rocking vibrational mode of water molecules.^[35]

Table 2: IR spectra bands of the SMX and its complexes

	SMX	Mn(II)	Ni(II)	Cu(II)	Zn(II)	La(III)	Nd(III)	Gd(III)	Y(III)
ν_{as} (NH):NH ₂	3468	3466	3464	3467	3476	3468	3470	3460	3450
ν_{s} (NH):NH ₂	3375	3378	3373	3374	3386	3379	3375	3372	3371
ν_{as} (NH): sulfonamide group	3298	3288	3287	3285	3295	3290	3292	3288	3290
ν_{s} (NH): sulfonamide group	3242	3250	3236	3219	3224	3238	3239	3249	3251
ν methaxazole ring.	1645	1650	1648	1649	1648	1650	1648	1649	1641
δ (NH ₂)	1623	1620	1619	1622	1623	1621	1620	1623	1623
ν (C=C): phenyl ring	1597 1504	1596 1502	1597 1504	1596 1504	1598 1502	1595 1505	1596 1503	1597 1503	1596 1502
ν_{as} (SO ₂): sulfonayl group	1365	1373	1376	1380	1385	1384	1375	1377	1380
ν_{s} (SO ₂): sulfonayl group	1188	1160	1150	1147	1148	1161	1150	1152	1148
C-N	1311	1270	1275	1285	1250	1271	1256	1266	1270
ν (M-O)	-	509	521	474	511	482	502	490	485
ν (M-N)	-	443	439	442	411	432	428	433	429
ν (M-Cl)	-	260	271	271	275	260	268	261	266

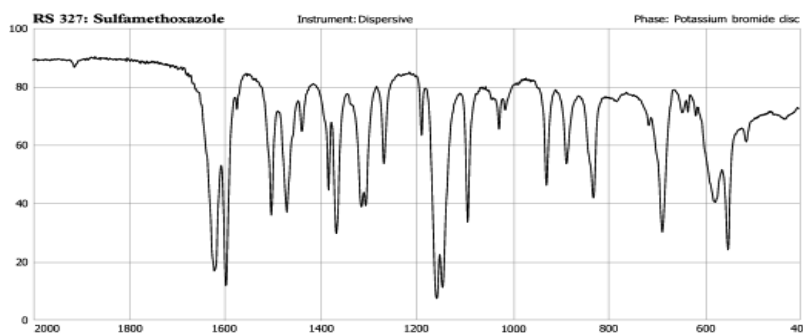


Fig.2: IR spectra of SMX ligand

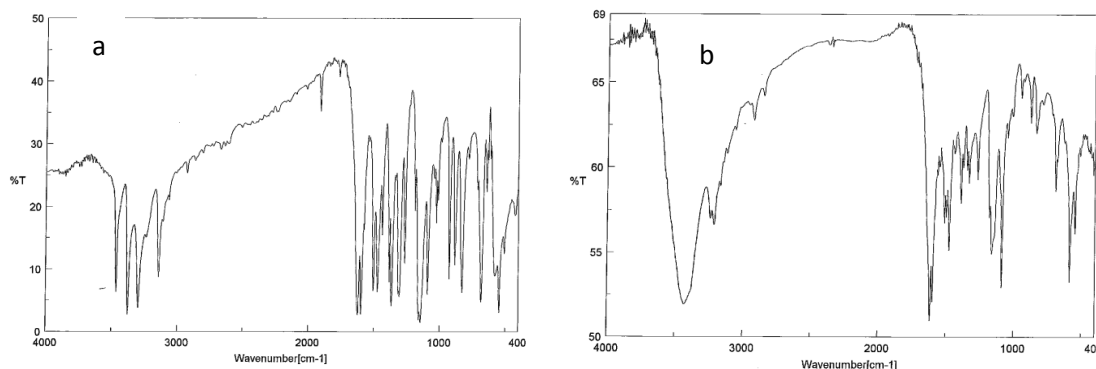


Fig.3: IR of La-SMX (a) and Cu-SMX (b) complexes

3.2 Electronic spectra and magnetic measurements

The UV-Vis. electronic absorption spectrum of the free SMX ligand (Figure 4a) exhibited two absorption bands in the ultraviolet region, the band at 47170 cm^{-1} assigned to the $\pi \rightarrow \pi^*$ transition for the intera-ligand of aromatic system C=C character and a strong absorption band at 37037 cm^{-1} is refer to $n \rightarrow \pi^*$ transition for oxygen atom of S=O group or nitrogen atom of $-\text{NH}_2$ and imine $-\text{N}=\text{C}-$ groups, respectively.^[36] Upon complexation, there are slight electronic changes of these bands due to the interaction of SMX ligand with Manganese(II), Nickel(II), Copper(II), zinc(II), Lanthanum(III), Neodymium(III), Gadolinium(III) and Yttrium(III) metal ions (Table 3). The observed magnetic momentum value of Cu(II) complex is 1.94 BM, falls within the range observed for octahedral geometry. Further, the electronic spectra of Cu(II) complex (Figure 4b) shows one broad peak at 17240 cm^{-1} due to transition between ${}^2\text{E}_g \rightarrow {}^2\text{T}_{2g}$ indicating octahedral geometry.^[37] Mononuclear Cu(II) complexes regardless of stereochemistry are expected to have effective magnetic moments in the range 1.9–2.2 B.M. usually higher than the spin only moment due to orbital contribution and spin-orbit coupling as validated by.^[38] Transitions attributed to metal to ligand charge transfer occur at 30303 cm^{-1} . The Ni(II) complex exhibits peaks at 14859, 17668 and 23866 cm^{-1} attributed to the ${}^3\text{A}_{2g}(\text{F}) \rightarrow {}^3\text{T}_{2g}(\text{F})$, ${}^3\text{A}_{2g}(\text{F}) \rightarrow {}^3\text{T}_{1g}(\text{F})$, and ${}^3\text{A}_{2g}(\text{F}) \rightarrow {}^3\text{T}_{1g}(\text{P})$ transitions respectively, suggests octahedral geometry. The magnetic moment value of Ni(II) complex is found to be 3.05 BM, falls within the range of 2.8-3.5 BM for octahedral complexes, suggesting octahedral geometry.^[39] The Mn(II) complex shows three absorption peaks at 14859 cm^{-1} expected for ${}^6\text{A}_{1g} \rightarrow {}^4\text{T}_{1g}(\text{S})$, at 19342 cm^{-1} corresponding to ${}^6\text{A}_{1g} \rightarrow {}^4\text{T}_{2g}(\text{G})$ and a broad band at 23923 cm^{-1} may be due to ${}^6\text{A}_{1g} \rightarrow {}^4\text{A}_{1g}$, suggesting octahedral geometry.^[40] Further, the octahedral geometry is proposed based on magnetic

moment. The magnetic moment of the complex is found to be 5.22 BM, falls within the range expected for octahedral geometry. The electronic spectrum of Zn(II) complex show one peak at 26247 cm^{-1} due to charge transfer from ligand to metal. The observed magnetic moment value for this complex is zero, indicating diamagnetic nature of the complex. It is expectedly showed no d-d transition because it had d^{10} configuration. On the basis of analytical, conductance and spectral data, octahedral geometry is assigned to zinc complex.^[41]

The complex formation with lanthanides metal ions resulted in a hypsochromic shift of the ligand bands of its electronic spectrum. The absorption bands of neodymium(III) (Figure 4d) in the UV and visible region appear due to transitions from the ground level ${}^4\text{I}_{9/2}$ to the excited J levels of 4f configuration.^[42] The sharp bands due to $f-f$ transition originating within the ${}^4f^n$ configuration of lanthanide ions are only slightly affected by the immediate surroundings of the metal ion, and this is commonly attributed to the shielded nature of the 4f orbital by the overlying $5s^2$ and $5p^6$ orbitals. However, the shift to lower frequency region can be concluded as due to complex formation.^[43] The shapes of hypersensitive transitions of the complexes closely resemble that of the seven coordinated complexes^[44], suggesting the coordination number seven around the metal ion in these complexes. The magnetic susceptibility values (Table 3) of the complexes reveal that the lanthanum(III) and yttrium(III) complexes are diamagnetic, while neodymium(III) and gadolinium(III) are paramagnetic. The magnetic susceptibilities of these two paramagnetic complexes, showed slight deviation from the van Vleck values^[45], indicating an insignificant participation of the 4f electrons in the bonding, since these are well shielded by $5s^2 5p^6$ octet.

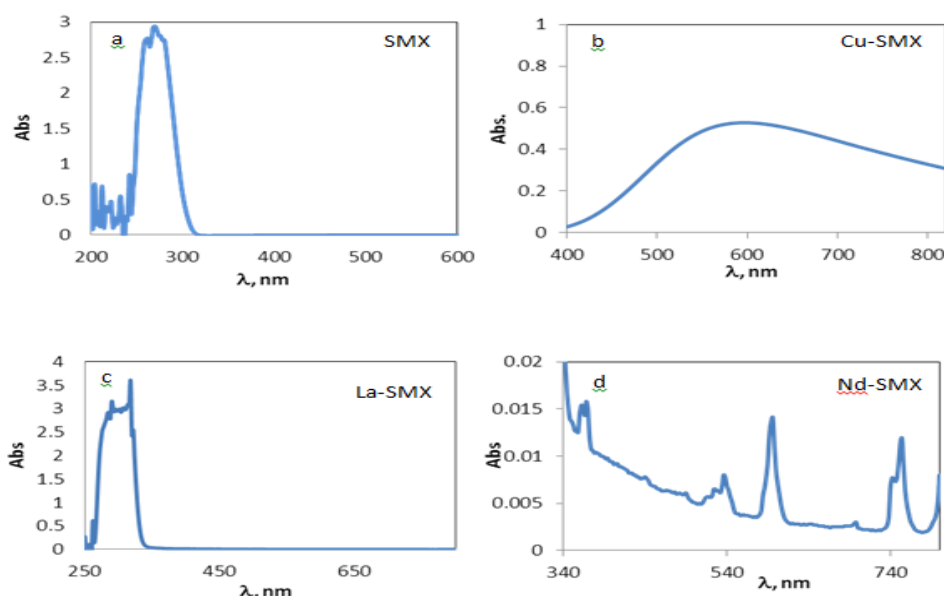


Figure.4: Electronic spectra of some SMX complexes

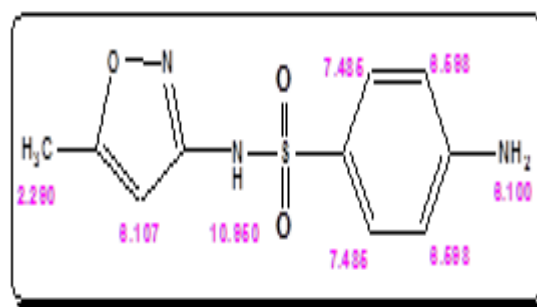
Table 3: Electronic spectral bands and magnetic moments of the SMX complexes

Compound	λ , nm	λ , cm^{-1}	Assignment	μ , B.M
SMX	212 270	47170 37037	$\pi \rightarrow \pi^*$ $n \rightarrow \pi^*$	-
[MnL ₂ Cl ₂].2H ₂ O	210 275 418 517 675	47619 36363 23923 19342 14837	$\pi \rightarrow \pi^*$ $n \rightarrow \pi^*$ ${}^6A_{1g} \rightarrow {}^4A_{1g}$ ${}^6A_{1g} \rightarrow {}^4T_{2g}(G)$ ${}^6A_{1g} \rightarrow {}^4T_{1g}(S)$	5.22
[NiL ₂ Cl ₂].3H ₂ O	212 272 419 566 673	47170 36765 23866 17668 14859	$\pi \rightarrow \pi^*$ $n \rightarrow \pi^*$ ${}^3A_{2g}(F) \rightarrow {}^3T_{1g}(P)$ ${}^3A_{2g}(F) \rightarrow {}^3T_{1g}(F)$ ${}^3A_{2g}(F) \rightarrow {}^3T_{2g}(F)$	3.05
[CuL ₂ Cl ₂].3H ₂ O	211 280 330 580	47393 35714 30303 17240	$\pi \rightarrow \pi^*$ $n \rightarrow \pi^*$ CT ${}^2E_g \rightarrow {}^2T_{2g}$	1.94
[ZnL ₂ Cl ₂].2H ₂ O	212 269 381	47170 37175 26247	$\pi \rightarrow \pi^*$ $n \rightarrow \pi^*$ CT	dia
[LaL ₂ Cl ₃].3H ₂ O	212 272	47170 36765	$\pi \rightarrow \pi^*$ $n \rightarrow \pi^*$	dia
[NdL ₂ Cl ₃].2H ₂ O	214 278 362 536 594 742	46729 35971 27624 18657 16835 13477	$\pi \rightarrow \pi^*$ $n \rightarrow \pi^*$ CT ${}^4I_{9/2} \rightarrow {}^4G_{9/2}$ ${}^4I_{9/2} \rightarrow {}^4G_{5/2}, {}^2G_{7/2}$ ${}^4I_{9/2} \rightarrow {}^2S_{3/2}, {}^4F_{7/2}$	3.68
[GdL ₂ Cl ₃].H ₂ O	212 272	47170 36765	$\pi \rightarrow \pi^*$ $n \rightarrow \pi^*$	7.79
[YL ₂ Cl ₃].3H ₂ O	210 275	47619 36363	$\pi \rightarrow \pi^*$ $n \rightarrow \pi^*$	dia

3.3 ¹H-NMR spectra

The ¹H-NMR spectra of the SMX free ligand has the expected distinguish signals. ¹H-NMR chemical shifts of SMX drug are assigned in Scheme 1. The ¹H-NMR spectra of [Zn(SMX)₂Cl₂].2H₂O and [Y(SMX)₂Cl₃].3H₂O complexes are shown in (Figure 5) and their chemical shifts are listed and assigned in (Table 4). The CH₃ proton shows singlet at $\delta = 2.290$ ppm and isoxazole proton at $\delta = 6.107$ ppm. In addition a multiplet peak at $\delta = 6.598$ and 7.485 ppm may be due to aromatic protons and peak at $\delta = 10.95$ ppm is due to NH proton. The -NH proton of sulfonamid group in case of Zn(II) and Y(III) complexes is disappears indicating the involvement of sulfonamid nitrogen in the coordination. Signals observed in the zinc(II) and yttrium(III) SMX complexes at region of $\delta = 3.329$ and

3.359 ppm, respectively are due to proton of uncoordinated water molecules.



Scheme 1. Proton positions and δ -chemical shift (ppm) of the free SMX ligand.

Table 4: ¹H NMR spectra for the SMX ligand and its zinc and yttrium complexes.

Assignments	δ (ppm)		
	SMX	Zn(II)	Y(III)
H; NH	10.950	-	-
H; isoxazole	6.107	6.012	6.080
H; aromatic	6.598, 7.485	6.572, 7.465	6.610, 7.466
H; NH ₂	6.100	6.053	6.095
H; H ₂ O	-	3.329	3.359
H; CH ₃	2.290	2.268	2.277

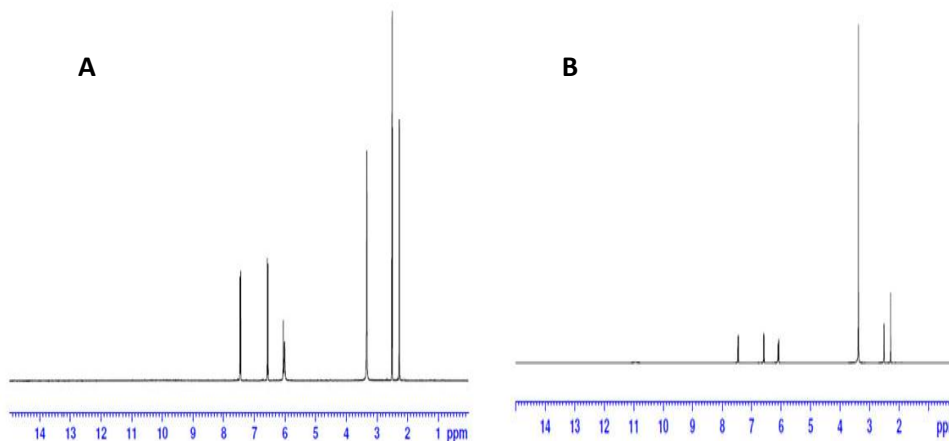


Figure 5: ¹H-NMR spectrum of [Zn(SMX)₂Cl₂].2H₂O(A) and [Y(SMX)₂Cl₃].3H₂O (B)

3.4 Structure of the Sulfamethoxazole complexes

The results obtained lead to the conclusion that sulfamethoxazole acts as a bidentate ligand complexing the metal ion through the sulfonyl oxygen and nitrogen of the amide group. The metal ion acquires a coordination number of six or seven. Based on the physicochemical

and spectral data obtained, an octahedral geometry was proposed for the transition metal(II) complexes(Fig 6A) and a monocapped trigonal prism geometry was proposed for the lanthanide(III) complexes, as shown in (Fig6B).^[46]

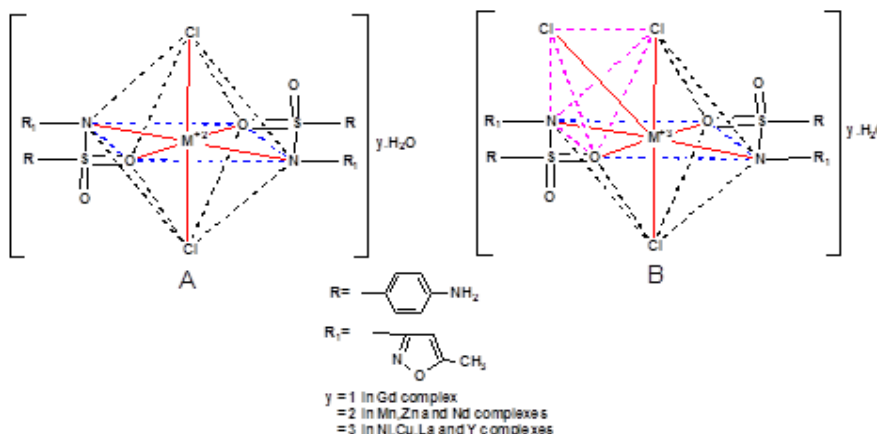


Figure.6: The geometry structures of sulfamethoxazole complexes.

3.5 Scanning electron microscopy

The microstructure, surface morphology and chemical composition of the free ligand (SMX) and its Nickel(II) and Gadolinium(III) complexes are studied using scanning electron microscopy. Typical scanning electron micrographs are shown in (Figure7). The surface morphology of SEM micrograph reveals the well sintered nature of the complexes with variant grain sizes and shapes. Figure 7 illustrates the SEM photographs of the free ligand and the synthesized SMX complexes. The uniformity and similarity in the particles size, shape and forms of the synthesized SMX complexes indicate that the morphological phases of Ni(II) and Gd(III) complexes have unhomogeneous matrix. SMX showed a plate like habit crystal, compact structures can be observed with irregular shapes and different sizes (Figure7a) and its average particle size is found to be 35µm. Clear and small

grains of a rectangular needle shape are noticed for the Ni-SMX complex, as shown in (Figure 7b). The inhomogeneous phase formation of the Ni(II) sulfamethoxazole complex is of small-to-medium particle size of different shape. The particle size distribution of this complex is evaluated and the average particle size is found to be 2.7µm, as exhibited in (Figure 7b). The photo (Figure 7c) shows particles of an irregular complex has an irregular shape and the adherence of the smaller particles to the solid surface of the larger particles. The average diameter of the small-to-medium variant particles is found to be 1.5 µm. It can be concluded that the significance of this result is in the conversion of geometric nano-particles of free sulfamethoxazole to smaller unhomogeneous nanoparticles upon the complexation with Ni(II) and Gd(III) ions.

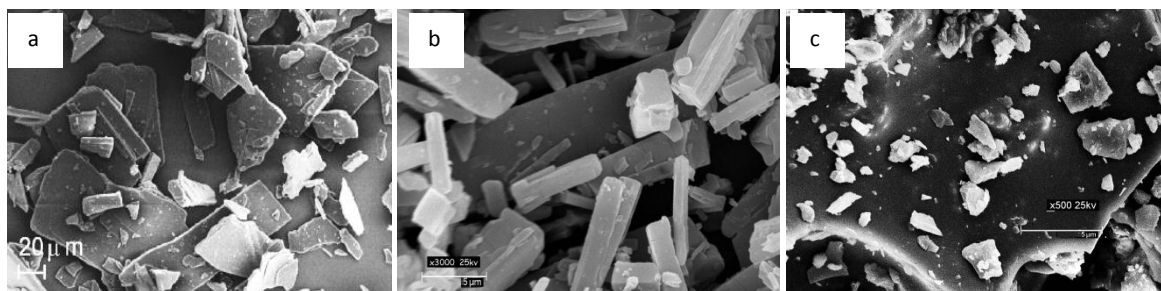


Figure 7: SEM micrograph of the free ligand sulfamethoxazole (a) Ni-SMX complex (b) and Gd-SMX complex (C).

3.6 X-ray powder diffraction

The X-ray powder diffraction patterns in the range of $10^\circ < 2\theta < 80^\circ$ for the free SMX ligand and its Mn(II), Ni(II), Cu(II), Zn(II), La(III), Nd(III), Gd(III) and Y(III) complexes were carried in order to obtain an idea about the lattice dynamics of the resulted complexes. X-ray diffraction of these compounds were recorded and shown in (Figure 8). The values of 2θ , d value (i.e. the volume average of the crystal dimension normal to diffracting plane), full width at half maximum (FWHM) of prominent intensity peak, relative intensity (%) and particle size of compounds were comprised in (Table 5). The crystallite size could be estimated from XRD patterns by applying FWHM of the characteristic peaks using Deby-Scherrer equation.^[47]

$$D = K\lambda / \beta \cos\theta$$

where D is the particle size of the crystal gain, K is a constant (0.94 for Cu grid), λ is the X-ray wavelength (1.5406 Å), θ is the Bragg diffraction angle and β is the integral peak width. The particle size was estimated relative to the highest value of intensity compared with the other peaks. X-ray powder diffraction patterns are carried out in order to obtain an idea about the lattice

dynamics of the complexes. By comparing of the obtained X-ray powder diffraction patterns given in Figure 8, the X-ray powder diffraction patterns throw slight only on the fact that each solid represents a definite compound of a definite structure which is not contaminated with starting materials. The identification of the complexes is performed by a known standard method.^[48] Such facts suggest that the prepared Mn(II), Ni(II), Cu(II), Nd(III), Gd(III) and Y(III) complexes are amorphous. On the other hand, the data give an impression that the particle size of the Zn(II) and of the La (III) complex located within nano-scale range. The XRD spectra of SMX and its complexes show that SMX is of a crystalline character, whereas its complexes appear to exhibit amorphous character and these are expected to possess enhanced bioavailability and improved tableting properties as compared with the parent drug.^[49,50] It is generally understood that crystalline materials exhibit high elasticity and brittleness when subjected to mechanical stress^[51]; therefore, it may be considered appropriate to introduce amorphous character by milling the ACT complexes before granulation and compression into tablets.

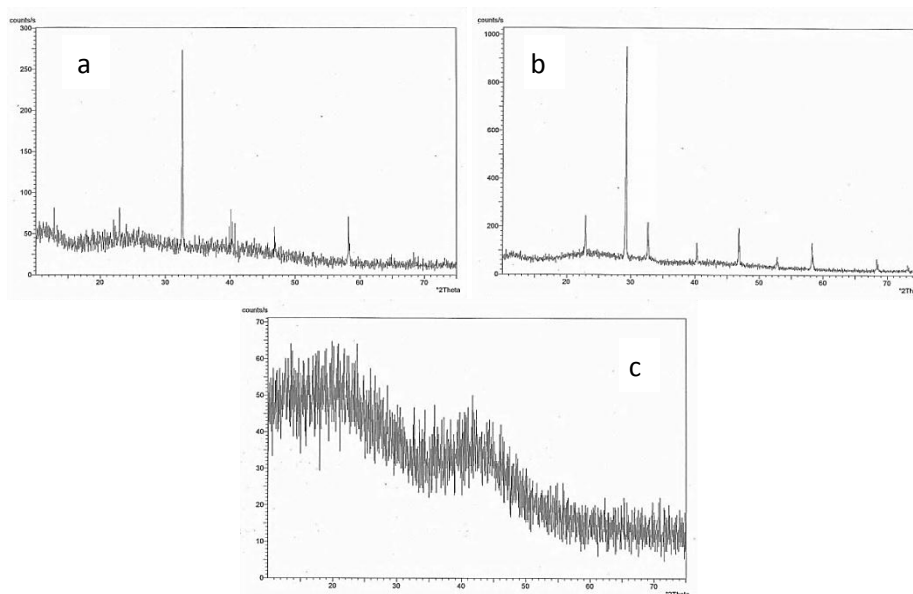


Figure 8: (a) XRD pattern of La-SMX, (b) Zn-SMX and (c) Mn-SMX complexes.

Table: 5 XRD spectral data of the highest value of intensity of some SMX complexes.

compound	2θ	FWHM	Relative intensity (%)	Particle size (nm)
La-SMX	32.763	0.001	100	132.2
Zn-SMX	29.122	0.001	100	131.0

3.7 Biological Screening

In vitro, the biological activities of the ligand and its metal complexes were screened for antibacterial against *E. coli* (ATCC 8739) and *S. aureus* (ATCC 6538), and for antifungal against *A. flavus* (ATCC 9643), *A. fumigatus* (ATCC 1022). The results of the antimicrobial activity of the ligand and its complexes against all tested bacterial and fungal strains are shown in (Table 6). Comparative study of the ligand and its metal complexes indicates that most of the metal complexes exhibit higher antimicrobial activity than that of the free ligand and the control (drug).^[52]

From these results, we can summarize that,. Generally, the active property of the free drug against the used strains is increased by complexation, except with Ni(II), Zn(II) and Y(III), it is reduced. The antifungal activity of these complexes is stronger than the antibacterial activity. The increasing behavior of the lipophilicity of these complexes seems to be responsible for their potent of antibacterial activity. Accordingly, these complexes deactivate various cellular enzymes, which play a vital role in various metabolic pathways of these microorganisms. It has also been proposed that the

ultimate action of the toxicant is the denaturation of one or more proteins of the cell, which as a result, impairs normal cellular processes. According to Overton's concept of cell permeability, the lipid membrane that surrounds the cell favors the passage of only lipid soluble materials due to which liposolubility is an important factor that controls antimicrobial activity. On chelating, the polarity of metal ion is reduced to a greater extent due to the overlap of the ligand orbital and partial sharing of the positive charge of the metal ion with donor groups. Further, it increases the delocalization of π -electrons over the whole chelates ring and enhances the lipophilicities of the complex. The increased lipophilicities of complexes permit easy penetration into lipid membranes of organisms and facilitates as blockage of metal binding sites in enzymes.^[53] This phenomenon was slightly increasing in the case of manganese due to its smaller ionic size and higher electronegativity. La(III) complex also, has shown promising antimicrobial activity against the four strains. We are optimistic that future studies on biological properties of this complex of Sulfamethoxazole may lead to the development of a new class of specific and effective pharmaceutical agents.

Table 6: Antimicrobial activity Sulfamethoxazole and its complexes

Compound	Antibacterial		Antifungal	
	<i>Escherichia coli</i>	<i>staphylococcus aureus</i>	<i>Aspergillus flavus</i>	<i>Aspergillus fumigatus</i>
SMX	2	17	20	25
[MnL ₂ Cl ₂].2H ₂ O	13	15	25	22
[NiL ₂ Cl ₂].3H ₂ O	2	8	19	22
[CuL ₂ Cl ₂].3H ₂ O	12	22	28	28
[ZnL ₂ Cl ₂].2H ₂ O	10	14	15	16
[LaL ₂ Cl ₃].3H ₂ O	33	29	35	27
[NdL ₂ Cl ₃].2H ₂ O	10	34	36	26
[GdL ₂ Cl ₃].H ₂ O	8	22	12	18
[YL ₂ Cl ₃].3H ₂ O	7	15	21	18

Diameter of inhibition zone in mm

The increase activity of the metal complexes can be explained on the basis of Overton's concept^[54,55] and Tweedy's chelation theory.^[56] Metal complexes also disturb the respiration process of the cell and thus block the synthesis of proteins, which restricts further growth of the organism.^[57] Finally, it is suggested that the reason for this higher antimicrobial efficacy could be related to the inhibition of several structural enzymes that play a key role in vital metabolic pathways of the microorganisms.

The ligand with nitrogen and oxygen donor system might inhibit enzyme production, since the enzymes which

requires these groups for their activity appear to be more liable to deactivation by metal ions upon chelation. The chelation reduces considerably the polarity of the metal ions in the complexes, which in turn increases the hydrophobic character of the chelate and thus enables its permeation through the lipid layer of microorganisms.^[58]

CONCLUSION

Sulfamethoxazole (SMX) drug complexes formulas with Mn (II), Cu (II), Ni (II), Zn (II), Y(III), La(III), Nd(III) and Gd(III) metal ions were synthesized and characterized by elemental analysis, molar conductance, magnetic susceptibility, UV-vis, IR and ¹H-NMR

spectroscopy. The data corroborated octahedral geometry for the divalent metal complexes and a mono capped trigonal prism geometry was proposed for the lanthanide(III) complexes. The conductance measurements in DMSO indicate nonelectrolytic nature of the complexes. The in-vitro antimicrobial studies of the complexes against *E. coli* (ATCC 8739) and *S. aureus* (ATCC 6538) and for antifungal against *A. flavus* (ATCC 9643) and *A. fumigatus* (ATCC 1022), showed that $[\text{LaL}_2\text{Cl}_3] \cdot 3\text{H}_2\text{O}$ had broad spectrum antimicrobial activities against all the microbes more than the other complexes.

ACKNOWLEDGEMENT

We thank the technical staff of Chemistry, Biochemistry and Microbiology Department of covenant University, Faculty of science Sana'a University, Yemen for their support during this research.

4. REFERENCES

- Guo, Z., Sadler P.J.: *Angew. Chem. Int. Ed.*, 1999; 38: 1512–1531.
- Klaus, F., *Analytical Profiles of Drug Substances*, 2nd Ed., Academic Press, TNC, 1984; 2: 467.
- Vree, T.B., Hekster, Y.A.: *Clinical Pharmacokinetics of Sulfonamides and Their Metabolites*, Karger: Basel, 1987.
- Vree, T.B., Hekster, Y.A.: *Pharmacokinetics of Sulfonamides Revisited*, Karger: Basel, New York, 1985.
- Monti, L., Ana Pontoriero N. M., Giulidori, C., Hure, E. and Patricia, A. M. W., Rodríguez, M. V., Feresin, G., Campagnoli, D. and Rizzotto, M. *Biometals*, 2010; 23: 1015-1028.
- Sharaby, C. *Inorg. Met. Org. Chem.*, 2005; 35: 133-142.
- Hambley, T.W.: *Dalton Trans*, 2007; 4929–4937.
- Orvig, C., Abrams, M.J.: *Chem. Rev.* 1999, 99, 2201–2203.
- Sadler, P.J., Zijian, G. *Pure Appl. Chem.*, 1998; 4: 863–871.
- Bruijninx, P.C.A., Sadler, P.J.: *Curr. Opin. Chem. Biol.*, 2008; 12: 197–206.
- Alias, M.F., Abdul Hassan, M.M., Khammas, S.J.: *Int. J. Sci. Res.*, 2015; 4: 2337–2342.
- Karthikeyan, G., Mohanraj, K., Elango, K.P., Girishkumar, K.: *Russ. J. Coord. Chem.* 2006, 32, 380–385.
- Mahind, L.H., Waghmode, S.A., Nawale, A., Mane, V.B., Dagade, S.P.: *J. Pharm. Bio. Sci.*, 2013; 5: 102–105.
- Mahmoud, W.H., Mohamed, G.G., El-Dessouky, M.M.I.: *Int. J. Electrochem. Sci.*, 2014; 9: 1415–1438.
- NasirUddin, M., Abdus Salam, Md., Sultana, *J. Mod. Chem.*, 2015; 3: 7–14.
- Ade, S.B., Kolhatkar, D.G., Deshpande, M.N.: *Int. J. Pharma Bio Sci.*, 2012; 3: 350–356.
- Tewari, B.B.: *Rev. Soc. Quím. Perú.*, 2011; 77: 144–151.
- Kaushal, R., Sheetal, Kaushal, R., Nehra, K.: *Int. J. Pharm. Pharm. Sci.* 2014; 6: 374–378.
- Thakur, G.A., Shaikh, M.M.: *Acta Pol. Pharm.*, 2006; 63: 95–100.
- Ferrer, S.; Borrás, J.; García-Esparia, E. *J. Inorg. Biochem.* 1990; 39: 297-305.
- Supuran, C.T.; Minicione, F.; Scozzafava, A.; Briganti, F.; Minicione, G.; Ilises, M.A. *Eur. J. Med. Chem.*, 1998; 33: 247-334.
- Blasco, F., Perello, L., Latorre, J., Borra, J. and Garcia Granda, S. *J. Inorg. Biochem.*, 1996; 61: 143-154.
- Blasco, F.; Ortiz, R.; Perello, L.; Borrás, J.; Amigo, J.; Debaerdemaeker, T. *J. Inorg. Biochem.*, 1994; 53: 117-126.
- Bellú, S.; Hure, E.; Trapé, M.; Rizzotto, M.; Sutich, E.; Sigrist, M.; Moreno, V. *Quim. Nova*, 2003; 26(2): 188-192.
- El-Nawawy, M.A., Farag, R.S., Sabbah, I.A., Abu-Yamin, A.M.: *Int. J. Pharm. Sci. Res.*, 2011; 2: 3143–3148.
- Topaçli, A., Kesimli, B.: *Spectrosc. Lett.*, 2001; 34: 513–526.
- British Pharmacopoeia TSO (The Stationery Office), v4.0.0. 2000.
- G. Svehla. *Vogel's Qualitative Inorganic Analysis*, seventh ed., 1996.
- Z. Szafran, R.M. Pike, M.M. Singh, *Microscale Inorganic Chemistry*, John Wiley, INC., New York, 1991.
- N. Kalyoncuoglu, S. Rollas, D. Sur-Altiner, Y. Yegenoglu, O. *Ang. Pharmazie*, 1992; 47: 769-774.
- Huheey, J. E., Keiter, E. A. & Keiter, R. L. *Inorganic Chemistry, Principles of Structure and Reactivity*, 4th ed. New York: Harper Collins College Publishers, 1993.
- Melina M., Fernando P., Paula C. de Souza, Clarice Q. Leite, Javier E., Otaciro R. Nascimento, Gianella F., María H. Torre. *J. Mol. Struct.*, 2013; 1036: 180–187.
- Robert M. Silverstein, Francis X. Webster and David J. Kiemle. *Spectrometric Identification of Organic Compound*, 7th ed. Jon-wiley. New York, 2005.
- Agarwal, S.K. and Tandon, J.P., *Monatsh. Chem.*, 1979; 110: 401-411.
- Nakamoto, K., *Infrared Spectra of Inorganic and Coordination Compounds*, New York: Wiley, 1963.
- Chohan, Z.H.; Shad, H.A.; Nasim F.H. *Organometal. Chem.*, 2009; 23(8): 319-328.
- Raman N, Ravichandran S and Thangarajan C. *J Chem Sci.*, 2004; 116: 215-219.
- Gulcan, M., Sonmez, M. and Berber, I. *Turk. J. Chem.*, 2012; 36: 189-200.
- Lever A B P, *Addiction and the Campus J Chem Edu.*, 1968; 45: 711-712.
- Sankhala D S, Mathur R C and Mishra S N, *Indian J Chem.*, 1980; 19A: 75-76.

41. Panchal P K, Parekh H M, Pansuriya P B and Patel M N, *J Enzyme Inhibit Med Chem.*, 2006; 21: 203-207.
42. S.S.L. Surana, M.Singh and S. N. Mishra; *J. Inorg. Nucl. Chem.*, 1980; 42: 61-65.
43. Jorgensen, C.K., The Nephelauxetic Series. *Prog. Inorg. Chem.*, 1962; 4: 73-124.
44. Sinha, S.P., *Spectrochim. Acta*, 1966; 22(1): 57-62.
45. Karakkar, D.G. *Inorg. Chem.*, 1967; 6(10): 1863-1868.
46. Van Vleck, J.H. and Frank, A.,. *Phys. Rev.*, 1929; 34: 1494-1495.
47. G. Karthikeyan, K. Mohanraj, K. P. Elango and K. Girishkumar, *Russ. J. Coordin. Chem.*, 2006: 32(5): 380-385.
48. C.X. Quan, L.H. Bin, G.G. Bang, *Mater. Chem. Phys.*, 2005; 91: 317-324.
49. B.D. Cullity, Elements of X-ray Diffraction, second ed., Addison-Wesley Inc., 1993.
50. H. Vromans, G.K. Bolhuis, C.F. Lerk, *Acta Pharm. Suec*, 1986; 23: 231-240.
51. T. Sebhatu, G. Alderborn Eu, *J. Pharm. Sci.*, 1999; 8: 235-242.
52. L.L. Augsburger, S.W. Hoag, Pharmaceutical Dosage Forms, Rational Design and Formulation, vol. 2, 3rd ed., Informapl, 2008; 73.
53. R.V. Prasad and N.V. Thakkar, *J. Molec. Catal.* 1994; 92(1): 9-20.
54. Xin Xinquan, Dai Anbang, *Pure Appl. Chem.*, 1988; 60(8): 1217-1224.
55. B.K. Gudasi, R.V. Shenoy, R.S. Vadavi, M.S. Patil, S.A. Patil, *Chem. Pharm. Bull.*, 2005; 53(9): 1077-1082.
56. Dharmaraj, N., Viswanathamurthi, P., Natarajan, K. *Trans. Met. Chem.*, 2001; 2:, 105-109.
57. Tweedy, B.G. *Phytopatho*, 1964; 55: 910-914.
58. Lau KY, Mayr A, Cheung KK. *Inorg Chim Acta*, 1999; 285(2): 223-232.
59. Z.H. Chohan, A.K. Misbahul and M.Moazzam, *Indi. J. Chemy A*, 1988; 27: 1102-1104.